Three-Dimensional Flow Studies on a Slotted Transonic Wind Tunnel Wall

J. M. Wu,* F. G. Collins,† and M. K. Bhat‡
The University of Tennessee Space Institute, Tullahoma, Tennessee

Three-dimensional flowfield measurements were made near a transonic slotted wall. Field velocity vectors and static pressure distributions have been obtained. The boundary-layer displacement thickness was found to vary in the transverse plane with its maximum at the slot centerline but decreased with increasing suction rate through the slot. The boundary-layer characteristics were sensitive to the mass transfer through the slot. The projection of the flowfield velocity vectors on the transverse plane revealed a vortex-like flow formation. The center of this secondary flow was located nearly at the edge of the wall shear layer and decreased in strength with applied suction. The secondary vortex motion may be attributed to the mean flow skewing, inhomogeneous transverse plane boundary layer, and the wall turbulence anisotropy. These sources produced rotation of opposite sense and their contributions varied with the suction rate.

Nomenclature

M	= Mach number
p	= pressure
$\tilde{p}$	$= p/q_\infty$
q	= dynamic pressure
Q	= volume flow rate through slot (applied)
Re	= freestream unit Reynolds number
U_e	= velocity at outer edge of shear layer
U_∞	= freestream velocity
u,v,w	= velocity components in x,y,z directions, respectively
u_τ	= friction velocity
u',v',w'	= turbulent fluctuation velocity components in x,y,z directions, respectively
$w_{z=\delta}$	= z component of velocity at edge of boundary layer above slot
w_{slot}	= z component of velocity at entrance to slot
x,y,z	= Cartesian coordinate system with origin at center of slot leading edge (see Fig. 2)
α	= angle of attack, or parameter in velocity/temperature relationship for an equilibrium turbulent boundary layer
δ	= boundary-layer thickness
δ^*	= displacement thickness
γ	= ratio of specific heats
ρ	= density
Subscripts	
e	= conditions at edge of boundary layer
t	= total condition
∞	= conditions in freestream

I. Introduction

TRANSONIC wind tunnels employ slotted or porous walls to relieve blockage and other interference effects. The slotted wind tunnel walls are known to be more efficient than porous walls in the subsonic speed range but neither type is completely effective. The problem of wall interference is further avoided by limiting the model size which reduces the blockage ratio. Under extreme conditions caused by testing thicker models and testing models at large angles of attack, etc., the wall interference can be significant even with slotted or porous walls. In addition, it is not economical to limit the blockage ratio to a very small value especially if large Reynolds numbers are desired. Therefore, the tendency in transonic wind tunnel testing is to increase the blockage ratio and, in the meantime, to reduce the wall interference, thereby improving the utility of a given wind tunnel. One of the practical methods to accomplish this is to control the flow near the wall so as to minimize the wall effect—the so-called adaptive wall technique.

The numerical procedures[1,2] used to estimate the wall interference or to design improved test section walls require conditions to be prescribed at the ventilated walls. These boundary conditions specify the pressure, streamline curvature, or flow velocity components, i.e., velocity vector, near the walls and perhaps the flow angle in the slot.[2] Hence, a detailed knowledge of the flowfield near the slotted tunnel wall is required. Although several studies have been performed on some aspects of the flow over slotted walls, the knowledge required for a complete understanding of the flow is not available.

Neyberg,[3] Berndt,[4] and Berndt and Sorensen[5] examined the flow through slots to formulate a homogeneous wall boundary condition for accurate numerical calculations of inviscid transonic flows around models in slotted test sections. The slot flow was examined with oil flow pictures of the flow through the slots and with pressure measurements made in and around the slots. Also, a special probe was used to measure the slot flow angle in the plenum chamber. For their experiments the test section pressure upstream of the model was greater than the plenum pressure and, consequently, there was an outflow from the test section into the plenum chamber. The flow entered the plenum chamber by entrainment and deflection. Near the model, and for a short distance downstream, the plenum pressure was greater than the test section pressure, thus causing inflow into the test section from the plenum chamber. The inflow into the test section was reported to be a mixed flow, consisting in part of fast air removed earlier (upstream) from the test section and of low momentum air from the plenum. This low momentum air formed a bubble which spread laterally and was driven farther into the wall boundary layer.[3] Based on the slot flow velocity measurements, Berndt[4] inferred that the viscous effects caused a 15% reduction in effective slot width for outflow from the test section. No measurements of the inflow into the test section were carried out.

Presented as Paper 82-0230 at the AIAA 20th Aerospace Sciences Meeting, Orlando, Fla., Jan. 11-14, 1982; submitted Jan. 22, 1982; revision received Oct. 15, 1982. This paper is declared a work of the U.S. Government and therefore is in the public domain.

*Professor, Aerospace Engineering and Director, Gas Dynamics Division. Associate Fellow AIAA.
†Professor, Aerospace Engineering. Member AIAA.
‡Graduate Research Assistant.

Matyk and Kobayashi[6] studied the boundary layer and cross flow characteristics of the Ames 2×2 ft and 11×11 ft transonic tunnel configurations. They reported that the boundary-layer displacement thickness downstream of the slots was approximately twice as large as that at the centerline of the solid portion between the slots. This result was attributed to the aspirating effect and was considered to be a result of the natural development of the slot boundary layer. The cross flow differential pressure drop across the slot was found to be nonlinear with mass outflow and the fluctuating component of the cross flow velocity was as large as 30%. Their measurements were obtained with a traversing straight pitot probe, and therefore, the complex three-dimensional nature of flow was not detected.

The boundary-layer displacement thickness has a strong influence on the slot cross flow characteristics. This becomes particularly significant due to the influence of the model-induced pressure variation on the development of the wall boundary layer. Furthermore, there are other slot flow problems that remain unanswered. Among these are the following: there are possibilities that the air returning to the test section contains vorticity and that there may be separation at the slot edges. The exact location of the surface where the plenum pressure exists in the slot flow is unknown. The cross flow may be too large for linearization, as is frequently assumed in the theoretical treatment. In spite of the vital role that the boundary layer on the slotted walls may play in understanding the features of the transonic wind tunnel wall flowfield, the experimental data on the flow near slotted walls is scarce and incomplete,[3-10] especially in view of the semi-three-dimensional nature of the flowfield in the presence of mass transfer across the slots.

In the present investigation a detailed study of the viscous flow phenomenon over a slotted wind tunnel wall was made. The experiments were carried out on a single slotted tunnel wall. Zigzag baffles with 14-deg slant angle were used to direct the flow in the slots. The tests were made with and without auxiliary suction through the slot. Due to the fact that the flow over a slotted wall is semi-three-dimensional in nature, a five port cone probe was used to measure the flow velocity through the wall boundary layer. The boundary-layer traverses were made above the slot and at three equally spaced transverse stations away from the slot. All the measurements were made at one longitudinal station. In addition, detailed pressure distributions in the neighborhood of the slot were obtained. No turbulence measurements were made and only mean quantities are reported in this study. A schematic of the measurement plane and flowfield is given in Fig. 1.

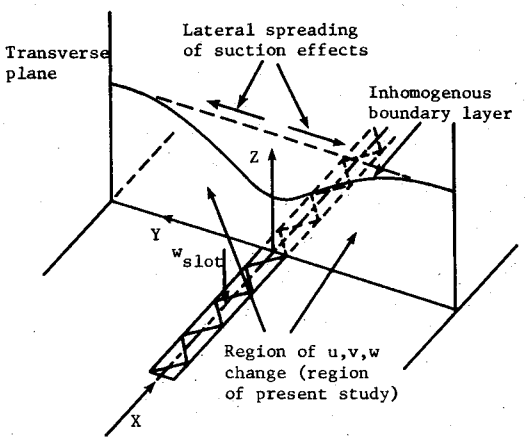

Fig. 1 Schematic of slot flow and measurement plane.

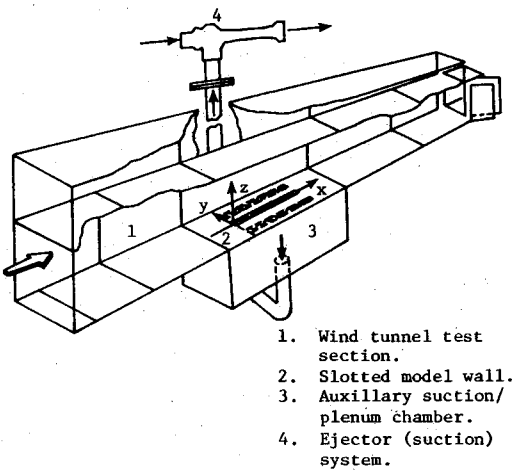

1. Wind tunnel test section.
2. Slotted model wall.
3. Auxillary suction/ plenum chamber.
4. Ejector (suction) system.

Fig. 2 Schematic of mounting of model wall on the tunnel floor.

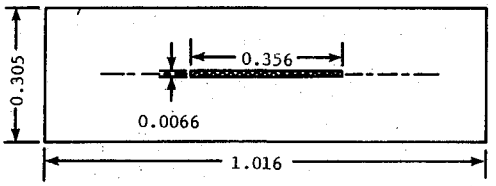

Fig. 3 Details of slotted model wall; all dimensions in meters.

II. Wind Tunnel Facility and Instrumentation

This experimental investigation was performed in the UTSI transonic wind tunnel. The tunnel is of the blow down type with a test section measuring 0.31-m wide×0.28-m high and 2.66-m long. The test section is topped along its entire length with a plenum chamber which is connected to the test section through a porous plate having about a 30% open area. No external suction or blowing was applied to the upper plenum.

A model of a section of a slotted wall test section, similar to that which exists in the 11×11 ft transonic tunnel at the NASA Ames Research Center, was constructed and mounted on the test section floor (Fig. 2). The model contained three slots, one on the tunnel centerline and one on each side, separated from the centerline by 0.051 m. Inserts could be placed in the slots to vary the number, length, and width of the slots. The present experiments were performed on a single slot of length 0.36 m and width 6.6×10^{-3} m (Fig. 3). Zigzag shaped baffles, making a 14-deg angle to the vertical, were placed in the slot.

A separate plenum chamber was provided below the slotted wall model. Suction to the chamber was provided by two air-operated ejector pumps. The suction rate was measured by a sharp-edge orifice plate flowmeter that was placed in the pipe. The meter discharge coefficient was taken from Ref. 11. The suction rate was varied by controlling the pumping media pressure with a dome controller. The flow rate was varied from 3.54×10^{-2} to 1.18×10^{-1} standard m^3/s (75 to 250 SCFM). Four rows of static pressure orifices facing the test section were installed on the plenum chamber plate. They ran longitudinally at the center of the solid portion between the slots and outside the slots, each at a distance of 2.54 cm from a slot centerline.

The purpose of this study (see Fig. 1) was to measure the three-dimensional velocity field that exists above a slot with suction. A five hole cone probe was used for this purpose. From each reading of the probe the local Mach number, static pressure, stagnation pressure, and flow direction were determined. Then, using an assumed form of the velocity-temperature relation for an equilibrium turbulent boundary layer, the flow velocity components were determined.

The small perturbation transonic analysis of Wu and Lock[12] and supersonic small perturbation theory[13] were applied to the cone-cylinder configuration to estimate its expected performance. Based on this calculation, it was decided to use a cone of 20-deg half-angle to have a suf-

ficiently large pressure difference across opposite sides and to place the surface orifices at 0.65 times the cone length from the tip, where the pressure was relatively constant. In general, it is desirable to have a probe with a constant but large sensitivity to be able to accurately measure small angular deflections [$S=\partial(\Delta p/p_t)/\partial\alpha$ per degree]. In the Mach number range of current interest (0.6-0.9) the sensitivity was predicted to be in the range of -0.008 to -0.011/deg. The method for using a five port cone to determine the local Mach number and flow angle is detailed in Refs. 14 and 15. The transonic small perturbation analysis of Wu and Lock,[12] which is known to have good agreement with experimental data, was used to numerically obtain the required cone probe calibration data.

To be able to determine the local velocity, either the local temperature has to be measured or a velocity-temperature relation for a turbulent shear layer has to be used. For the present measurements the latter technique was used in lieu of temperature measurements, even though the result should only be approximate because the viscous layer was not an equilibrium turbulent boundary layer. The velocity ratio is given by

$$\frac{V}{V_e}=\frac{M}{M_e}\left(\frac{T}{T_e}\right)^{1/2}$$

where the subscript e indicates the condition at the edge of the boundary layer. Then, the relationship between T/T_e and V/V_e from Ref. 16 was solved iteratively with the preceding expression to obtain the local velocity. The mixed Prandtl number was assumed to be 0.88, the parameter α was taken to be 25, and the wall was assumed to be adiabatic. The velocity components u, v, w then were obtained from the total velocity V, and the flow angles θ and ϕ. The presence of the baffle contributes to the asymmetry of the flowfield on either side of the slot.

The technique just described yields flow angles and velocity components relative to the axis of the cone probe. However, there were always misalignments in the mounting of the cone probe such that the cone coordinate system did not coincide with the tunnel coordinate system. For each probe mounting a test run, with a traverse made on a flat plate on the lower wall (all slots plugged), was made to determine the alignment error. Then a transformation was made from the cone axis to the tunnel axis.

The cone probe holder was fastened on a longitudinal traverse mechanism that was mounted inside the lower plenum chamber. It could be positioned at any longitudinal location by means of a lead screw; all the present measurements were made at a longitudinal station $x=19$ cm measured from the slot beginning. The probe holder was positioned under one of the closed slots and could be moved vertically with an electrical motor through a fitting on the slot. Using extension pieces, the cone probe could traverse over one of the open slots or 1.3, 2.5, or 3.8 cm transversely away from the slot.

All pressure and temperature measurements were digitized and stored in a microcomputer for later analysis. During one vertical scan of the cone probe away from the wall 96 measurements were made.

III. Results

The results to be reported here were obtained from a single slot, located on the tunnel centerline, at various test conditions. The tests were performed at Mach numbers of approximately 0.6, 0.76, and 0.9. The unit Reynolds number

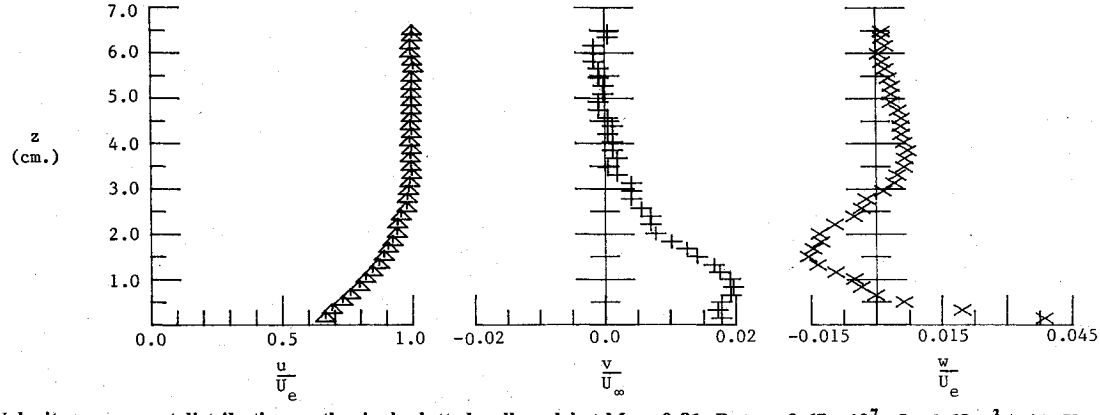

Fig. 4 Velocity component distribution on the single slotted wall model at $M_\infty \simeq 0.81$, $Re/m \simeq 2.67\times10^7$, $Q \simeq 1.65$ m^3/min, $Y=-1.27$ cm.

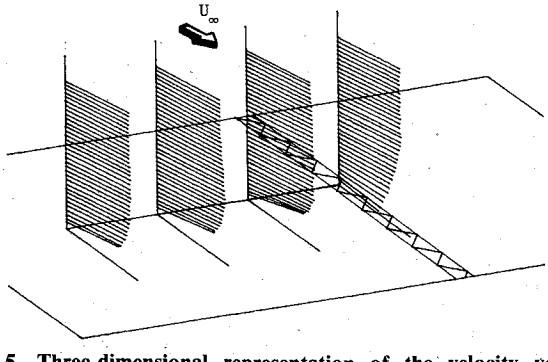

Fig. 5 Three-dimensional representation of the velocity vector distribution in the transverse plane of measurement for flow over the single slotted wall model at $M_\infty \simeq 0.76$ and $Re/m \simeq 3.4\times10^7$ (no applied suction, i.e., natural ventilation only).

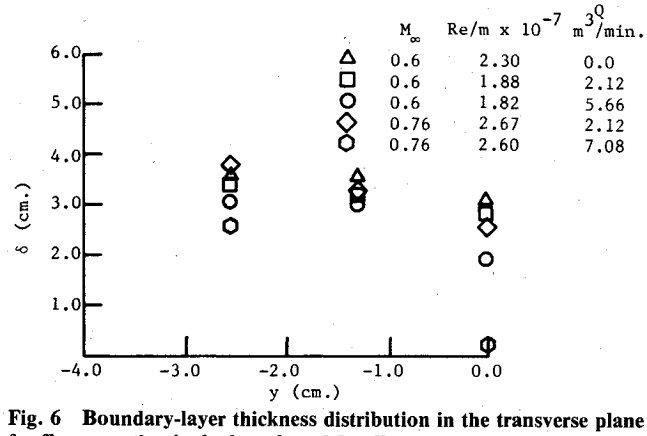

Fig. 6 Boundary-layer thickness distribution in the transverse plane for flow over the single slotted model wall.

varied from 1.6 to 3.1×10^7/m. The applied suction through the slot varied from zero (lower plenum valve closed), to moderate (3.54×10^{-2} m^3/s or 75 SCFM) and to high (0.118 m^3/s or 250 SCFM). For all the tests the cone probe was traversed in the z direction at a fixed x station of 19 cm and at four y stations (0, 1.3, 2.5, and 3.8 cm) (see Fig. 2).

The velocity component u, v, w in the x, y, z directions, respectively, were obtained from the cone probe measurements. A typical result for one cone probe traverse is shown in Fig. 4. The nature of the wall shear layer and the near region external to the shear layer was analyzed using these measured velocity components. It should be noted that in the immediate neighborhood of the wall (approximately 1.5-probe diameters) the cone probe results become spurious due to the probe-wall interference.

An example of the three-dimensional velocity profiles that were measured at the four transverse stations for one test condition is given in Fig. 5. The results were from four independent test runs but the test conditions were approximately the same. These plots exhibit the three-dimensional nature of the flowfield on the single slotted model wall in a qualitative sense. From these results it can be seen that the transverse and normal velocity components were skewed toward the slot for measurement stations away from the slot. The extent of the skewness decreased with distance away from the slot. The just described nature of the velocity vector distribution was observed over the entire experimental Mach number range ($M_\infty = 0.6$-0.9). Due to relatively small magnitude of v and w velocity components compared to the principal flow direction u velocity component and also because of the mode of presentation, the v and w velocity components are not explicitly revealed in Fig. 5. There was flow outward from the test section through the slot to the plenum chamber at this longitudinal measuring station for all the present measurements, even without applied suction (i.e., natural ventilation only). At the slot itself the flow was directed into the slot by the baffles. The baffle angle was 14 deg and the measured flow angle on the slot was slightly greater than 14 deg. The details of determining the velocity vectors using the cone probe measurements are outlined in Ref. 17.

The boundary-layer thickness was defined as the z location where the u component of the velocity was equal to 0.99 U_e, where U_e is the u component of the velocity at the edge of the boundary layer. The displacement thickness was defined as

$$\delta^* = \int_0^{z_e} \left(1 - \frac{\rho u}{\rho_e U_e}\right) dz$$

This is only an approximation to the actual displacement thickness for the three-dimensional flow.[18] It is estimated that the neglect of the v and w components led to a slightly overestimated value of δ^*.

The distribution of the boundary-layer thickness in the transverse (measurement) plane is shown in Fig. 6 for flow at two Mach numbers. The boundary-layer thickness remained relatively constant with no applied suction through the slot but decreased in the vicinity of the slot with applied suction and almost disappeared above the slot at the highest suction rate. The displacement thickness over the slot also decreased significantly with increase in applied suction rate.

The boundary-layer displacement thickness distributions in the transverse plane are shown for various Mach numbers and suction rates in Fig. 7. For no auxiliary suction δ^* decreased monotonically with increase in distance away from the slot axis except at the lowest Mach number. At $M_\infty = 0.6$ the natural suction velocity ($Q = 0.0$) is larger than at higher Mach numbers because the wall boundary layer is thicker than at the higher Mach numbers and this results in a lower downstream test section pressure with a consequently larger outflow from the test section into the plenum upstream on the slot at the measuring station. Matyk and Kobayashi[6] measured δ^* on the

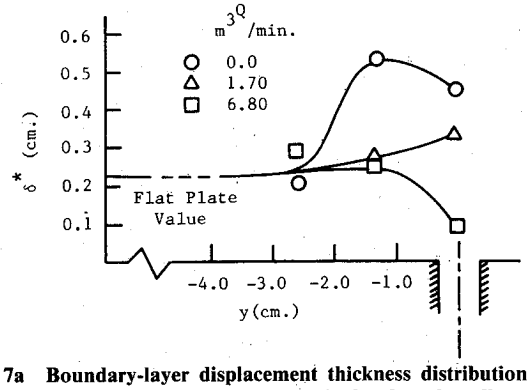

Fig. 7a Boundary-layer displacement thickness distribution in the transverse plane for flow over the single slotted wall model at $M_\infty \simeq 0.6$ and $Re/\text{m} \simeq 2.1 \times 10^7$.

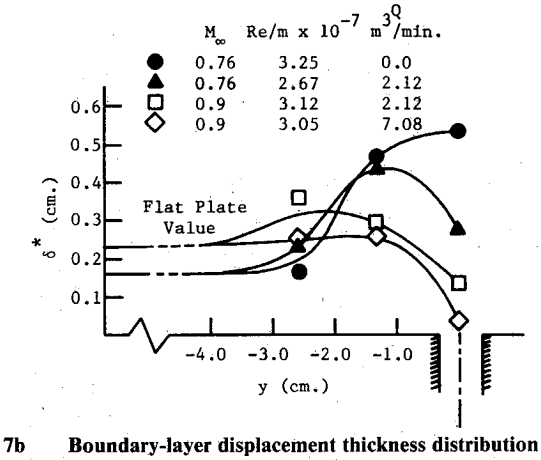

Fig. 7b Boundary-layer displacement thickness distribution in the transverse plane for flow over the single slotted wall model.

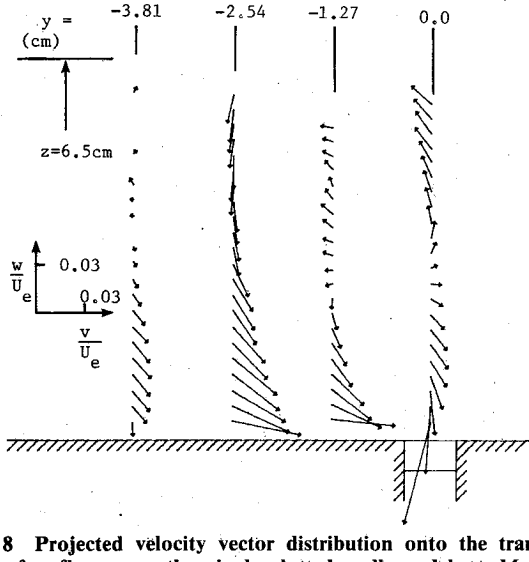

Fig. 8 Projected velocity vector distribution onto the transverse plane for flow over the single slotted wall model at $M_\infty \simeq 0.6$, $Re/\text{m} \simeq 2.4 \times 10^7$ with no applied suction ($Q \simeq 0.0$ m^3/min). The x component of velocity is directed out of the plane of paper.

slat between two slots and downstream of a slot and found that δ^* downstream of the slot was twice that of the value between the slots. The same type of variation of δ^* is observed in the present measurements but at one longitudinal location.

The reason for the increase in δ^* in the vicinity of the slot can be explained as follows. The boundary layer on a slotted wall is similar to the boundary-layer flow on a solid plate which contains a long, deep cavity. For no applied suction (with only natural ventilation) the flow entering into the plenum chamber is mostly drawn from the low momentum

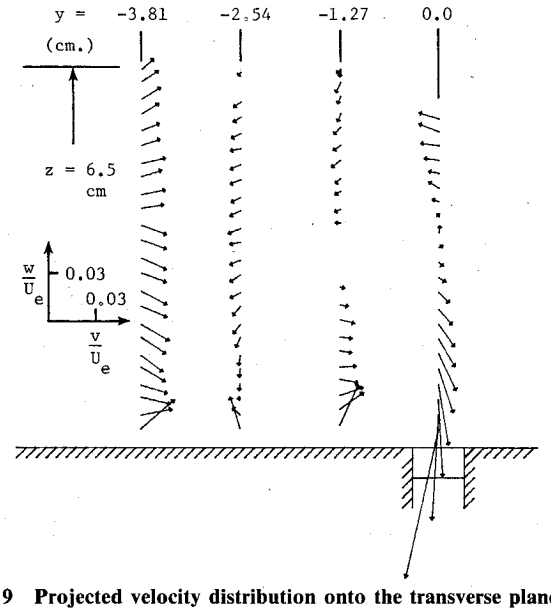

Fig. 9 Projected velocity distribution onto the transverse plane for flow over the single slotted wall model at $M_\infty \simeq 0.6$, $Re/m \simeq 1.89 \times 10^7$ with moderate applied suction ($Q \simeq 2.01$ m^3/min). The x component of velocity is directed out of the plane of paper.

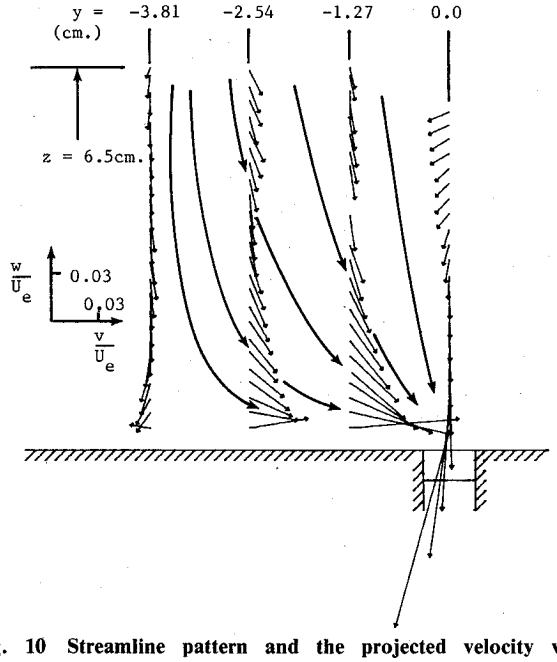

Fig. 10 Streamline pattern and the projected velocity vector distribution onto the transverse plane for flow over the single slotted wall model at $M_\infty \simeq 0.6$, $Re/m \simeq 1.78 \times 10^7$, $Q \simeq 7.1$ m^3/min. The x component of velocity is directed out of the plane of paper.

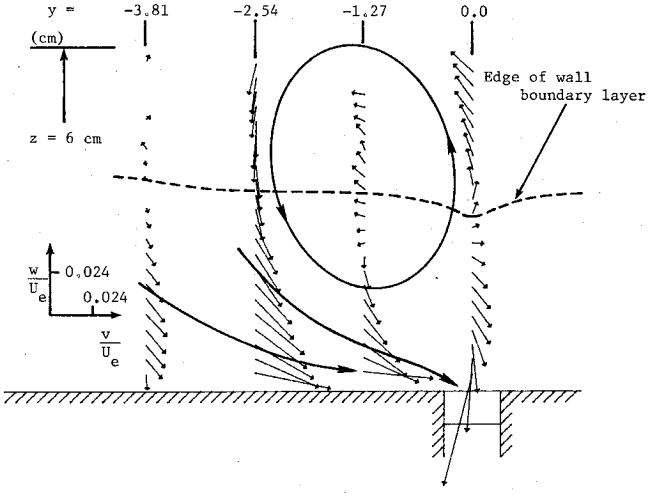

Fig. 11 Schematic of the secondary motion superimposed on the projected velocity vector distribution on the transverse plane of flow over the single slotted wall model at $M_\infty \simeq 0.6$, $Re/m \simeq 2.4 \times 10^7$ with no applied suction ($Q \simeq 0.0$). The x component of velocity is directed out the plane of paper.

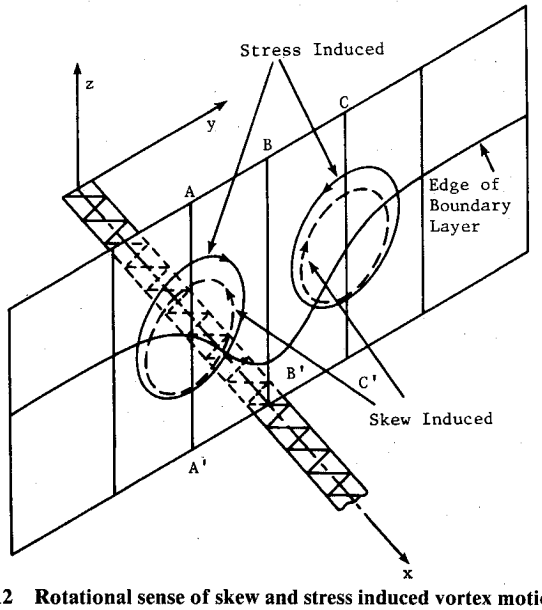

Fig. 12 Rotational sense of skew and stress induced vortex motion in transverse plane.

slotted wall boundary layer and very little comes in from the outer stream. This view is supported by the fact that δ varied only slightly away from the slot for $Q=0$ (Fig. 6). The drawing of mass from the boundary layer together with only a slight change in δ for zero to a moderate amount of applied suction through the slot results in an increased velocity defect in the shear layer and, consequently, an increase in δ^*. With applied suction the displacement thickness above the slot is reduced and the influence of the suction spreads laterally as the suction rate is increased.

The behavior of the flowfield is better visualized by considering the projection of the resultant of the v and w velocity components onto the transverse plane (Figs. 8-10). In these figures the main flow direction is out of the plane of the paper. The indicated velocities closest to the solid wall are in error due to the wall interference effect upon the cone probe. Nevertheless, significant secondary velocities were clearly observed away from the wall as a function of applied suction rates.

For test runs on a flat plate at Mach numbers 0.61 and 0.72 the measured magnitudes of v/U_∞ and w/U_∞ were less than 0.015 when the probe was free of wall interference. The maximum error in the measurement of cone probe pressures was estimated to be 1%. The corresponding changes introduced into the reduced velocity components due to these errors were not large enough to produce any discernable changes in the magnitude and orientation of the plotted velocity vectors in Figs. 8-10.

The flow pattern in the transverse plane exhibited in Figs. 8-10 indicates the existence of a vortex-like secondary flow. On close examination it is seen that, for no applied suction (only with natural ventilation), the vortex-like flow is strong and spread to the outer regions of the measurement plane which are outside the wall shear layer (Fig. 11). Close to the slotted wall the flow is directed toward and into the slot. At moderate suction the vortex-like tendency of the outer flow is rather

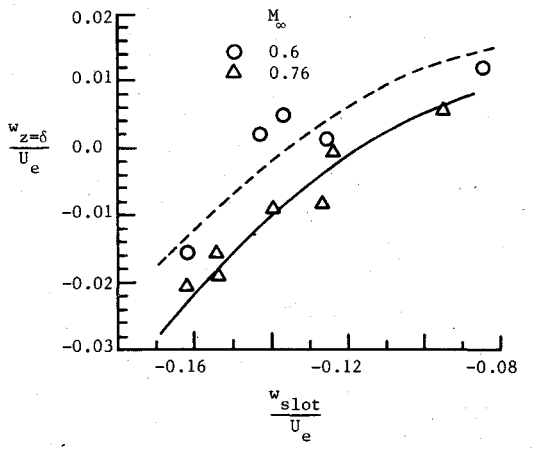

Fig. 13 Comparison of measured normal velocity at slot and at the edge of the boundary layer (at $y \simeq 0.0$ station in transverse plane) for the flow over a single-slotted wall model.

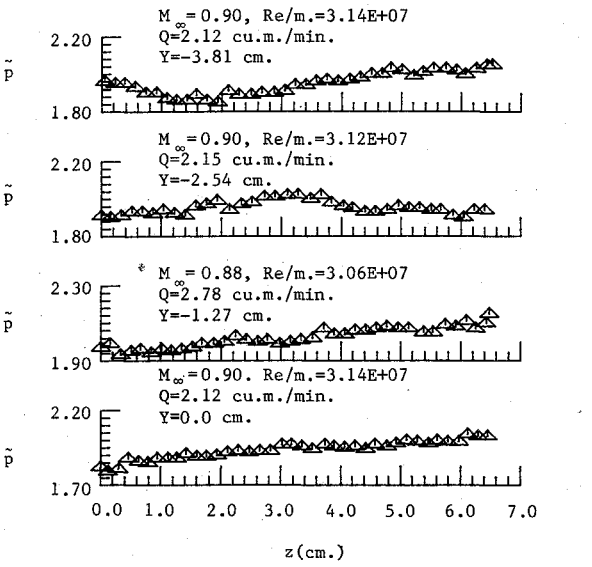

Fig. 14 Normalized static pressure distribution across the boundary layer on a single-slotted wall model.

decreased (Fig. 9) and at high suction this phenomenon has almost disappeared (Fig. 10). As mentioned earlier, at the highest suction rate the boundary layer almost disappeared over the slot. Therefore, it can be inferred that this secondary vortex flow can be attributed to an irregularity of the boundary-layer induced flow.

In the present experiments slots with rectangular ends were used. It is plausible that the vortices were generated from the slot lip as a consequence of the flow into the slot and that they then propagated outward from the wall while traveling downstream. However, such vortices should become stronger with increased suction rate through the slot but this was not the case for the present observations.

Secondary flow can arise in turbulent flows from mean flow skewing (secondary flow of the first kind) and from anistropy of the wall turbulence in the presence of a boundary layer which is nonuniform in the transverse direction (secondary flow of the second kind). Perkins[19] used the time-averaged streamwise vorticity equation for steady incompressible constant-property flow to examine the sources of streamwise vorticity in turbulent flow. Following the analysis of Perkins it is possible to explain the formation and the subsequent attenuation with increased applied suction of the secondary vortex flow observed in the present experiments.

The streamwise vorticity production rate due to mean flow skewing, labeled term P_1 by Perkins,[19] is given by

$$P_1 = \frac{\partial u}{\partial z}\frac{\partial v}{\partial x} - \frac{\partial u}{\partial y}\frac{\partial w}{\partial x}$$

For the present problem $\partial v/\partial x$ and $\partial w/\partial x$ are of the same order of magnitude while $\partial u/\partial z > \partial u/\partial y$ over most of the shear layer at moderate applied suction. While $\partial u/\partial y$ increases with increased applied suction there is a corresponding increase in $\partial u/\partial z$ due to a decrease in δ. Flow is always removed from the slot at the longitudinal station examined, even for no applied suction. This produces a lateral convergency of the streamlines toward the slot and nonzero values of $\partial v/\partial x$ exist which have opposite signs on opposite sides of the slot. The generation of streamwise vorticity by this mean flow skewing leads to a pair of vortices which expel fluid from the shear layer out into the mean flow. This mechanism of streamwise vorticity generation is explained in more physical terms in Fig. 11. With no applied suction the mean flow skewing source is dominant. The flow moves downward and toward the slot, except near the wall where it must move parallel to the wall. Because of the low momentum in the wall shear layer, the influence of the slot suction is greatest near the wall. However, since the amount of removed air is very small with no applied suction, only that portion of the flow near the wall is removed and that above it meets the air coming from the other side of the slot and moves upward, forming the secondary flow pattern shown. Note that the center of the secondary motion is far removed from the region of the boundary layer as it was defined previously.

The only significant stress induced streamwise vorticity production rate, labeled P_3 by Perkins,[19] is given by

$$P_3 = \frac{\partial^2}{\partial y \partial z}(\overline{v'^2} - \overline{w'^2})$$

where v' and w' are fluctuating velocity components. Based on measurements in several nonuniform, nominally two-dimensional viscous layers, Perkins showed that the difference of the Reynolds stresses in the transverse plane can be represented by the correlation

$$\frac{(\overline{v'^2} - \overline{w'^2})}{u_\tau^2} = F\left(\frac{z}{\delta}\right) = \left(1 - \frac{z}{\delta}\right)$$

which applies in the present geometry. Using this correlation the P_3 term becomes

$$P_3 = -\frac{u_\tau^2}{\delta}\left[\frac{2}{u_\tau}\frac{\partial u_\tau}{\partial y} - \frac{1}{\delta}\frac{\partial \delta}{\partial y}\right]$$

Although the preceding correlation was developed for incompressible flows, compressibility should not change the direction of the secondary motion. Consider the viscous layer over the slotted wall model which is inhomogeneous in the transverse plane, as shown in Fig. 12. In planes such as B-B', $\partial u_\tau/\partial y = \partial\delta/\partial y = 0$ which means that P_3 is zero. In planes such as A-A', $\partial u_\tau/\partial y > 0$ and $\partial\delta/\partial y < 0$ which means that P_3 is less than zero for negative y. Likewise, P_3 is positive for positive y. This leads to a secondary motion in a sense opposite to that produced by mean flow skewing.

Another plausible explanation for the disappearance of secondary motion with moderate suction (Fig. 9) is that the upward movement along the centerline from the secondary motion caused by mean flow skewing (Fig. 11) was balanced by the downward movement toward the slot caused by the increased suction. Only further experimentation can unambiguously determine the source of the streamwise vorticity that is observed and its change with amount of applied suction.

The conclusion is that the two sources of streamwise vorticity generate secondary motion of the opposite rotation sense, for the present geometry, which tend to counterbalance each other. At no applied suction, since there is only a slight variation of δ with y, the contribution to the secondary flow is mainly from the mean flow skewing (Fig. 11). With moderate applied suction the influence of the inhomogeneous boundary layer is strong and the two secondary flow sources tend to cancel one another. Then no secondary pattern is discernable (Fig. 9). At the highest applied suction rate the suction effect overrides the secondary motion and the velocity vectors are directed toward the slot (Fig. 10).

A comparison of the measured normal velocity component above the slot, w_{slot}, with that at the edge of the boundary layer above the slot, $w_{z=\delta}$, is shown in Fig. 13. As the suction was increased the w velocity component at the edge of the boundary layer reduced monotonically. In the layer close to the slot it was negative, i.e., the flow was directed into the slot, but w was still positive at the outer part of the boundary layer until w_{slot} was increased to a certain value. Then the entire shear layer was directed into the slot at the measured longitudinal location. At large suction the boundary layer almost disappeared.

The static pressure distributions through the viscous layer were measured at the same four locations where the velocity was measured. Typical results are given in Fig. 14 where $\bar{p}=p/(\frac{1}{2}\gamma p_\infty M_\infty^2)$. Above the slot the pressure always increased into the freestream but the measurements at the three other transverse locations did not show a definite trend at all Mach numbers.

IV. Conclusions

The following conclusions can be drawn from the present measurements made in a transverse plane of the turbulent flow over a flat single-slotted wall model, with and without applied suction, over the Mach number range 0.6-0.9 and a unit Reynolds number range 1.6 to 3.1×10^7/m.

1) The flowfield was found to be three-dimensional in nature with the flow velocity component inclined with the mainstream well beyond the conventionally defined boundary layer.

2) The flow pattern in the transverse plane indicated the existence of a vortex-like secondary flow that contained streamwise vorticity. It is plausible that the streamwise vorticity was created by mean flow skewing and by stress induction. For the present geometry the two sources created streamwise vorticity of opposite rotational sense. At low applied suction rates the mean flow skewing source dominated and created streamwise vorticity that was external to the normally-defined boundary layer. At moderate applied suction rates the two sources balanced each other and the secondary motion disappeared. At high applied suction rates the suction effect diminished the secondary motions and the velocity vectors were directed toward the slot.

3) The natural ventilation through the slot (no applied suction) was found to have an important influence upon the displacement thickness and the character of the three-dimensional flowfield above the slot. Both the boundary-layer and displacement thickness distributions in the direction transverse to the slot were very sensitive to the applied suction rate through the slot. The boundary-layer thickness was relatively constant in the transverse direction for no applied suction but decreased in the region of the slot with increased applied suction. The displacement thickness initially was considerably greater over the slot than away from it because of the natural suction at the transverse plane examined (see Fig. 7), but diminished rapidly with increased applied suction rate. The boundary layer was almost removed over the slot at high suction rates.

4) The ratio of the normal flow component (w) at the slot and at the edge of the boundary layer above the slot showed a nonlinear variation (Fig. 13). $w_{z=\delta}$ can be either positive or negative depending on the rate of suction. An accurate knowledge of this relationship is required for determining the wall boundary conditions for the numerical calculations. It appears that the streamwise variation of this relationship may be very complicated due to the three dimensionality of the flowfield.

5) Additional experiments need to be performed before the wall boundary condition, which is appropriate for calculations of flows about models in transonic tunnels with slotted walls, can be determined. These include measurements at additional transverse planes, with blowing rather than suction through the slot and with a multiple-slot wall. In addition, although several plausible explanations have been given for the observed secondary motion, measurements of the turbulent structure are required before the actual source of the motion will be known.

Acknowledgments

This work was supported under NASA University Grant NSG 2379 with NASA Ames Research Center, Moffett Field, Calif. The authors wish to thank Mr. Frank Steinle for his support of this work.

References

[1] Barnwell, R. W., "Improvements in the Slotted-Wall Boundary Condition," *Proceedings of the AIAA 9th Aerodynamic Testing Conference*, Arlington, Tex., June 1976, p. 21.

[2] Barnwell, R. W., "Design and Performance Evaluation of Slotted Walls for Two Dimensional Wind Tunnels," NASA TM 78 648, Feb. 1978.

[3] Neyberg, S. E., "Some Results from an Investigation of the Slot Flow in a Transonic Slotted Test Section Wall," AGARD CP 187,4B, April 1976.

[4] Berndt, S. B., "Transonic Flow at a Slotted Test Section Wall," AD A035308, AFOSR-TR-0035, Feb. 1977.

[5] Berndt, S. B. and Sorensen, H., "Flow Properties of Slotted Walls for Transonic Test Sections," AGARD CP 174, Paper 17, 1975.

[6] Matyk, G. E. and Kobayashi, Y., "An Experimental Investigation of Boundary Layer and Cross-Flow Characteristics of the Ames 2- by 2-Foot and 11- by 11-Foot Transonic Wind Tunnel Walls," NASA TM 73257, Dec. 1977.

[7] Everhart, J. L. and Barnwell, R. W., "A Parametric Experimental Study of the Interference Effects and the Boundary Condition Coefficient of Slotted Wind Tunnel Walls," AIAA Paper 78-805, 1978.

[8] Chen, C. F. and Mears, J. W., "Experimental and Theoretical Study of Mean Flow Boundary Conditions at Perforated and Longitudinally Slotted Wind Tunnel Walls," Arnold Engineering and Development Center, TR-57-20, 1957.

[9] Baronti, P., Ferri, A., and Weeks, T., "Analysis of Wall Modifications in a Transonic Wind Tunnel," Advanced Technology Laboratories, TR-181, 1973.

[10] Steinle, F. W. Jr. and Dougherty, N. S. Jr., private communication, NASA Ames Research Center, Moffett Field, Calif.

[11] Bean, H. S., ed., ASME Research Committee on Fluid Meters, "Fluid Meters: Their Theory and Application," 6th ed., ASME, New York, 1971.

[12] Wu, J. M. and Lock, R. C., "A Theory for Subsonic and Transonic Flow Over a Cone—With Small Yaw Angle," U.S. Army Missile Command, Tech. Rept. RD-74-2, Dec. 1973.

[13] Carafoli, E., *High-Speed Aerodynamics (Compressible Flow)*, Pergamon Press, London, 1956.

[14] Vahl, W. A. and Weirich, R. L., "Calibration of 30° Included-Angle Cone for Determining Local Flow Conditions in Mach Number Range 1.51 to 3.51," NASA TN D-4679, 1968.

[15] Norris, J. D., "Calibration of Conical Pressure Probes for Determination of Local Flow Conditions at Mach Numbers from 3 to 6," NASA TN D-3076, 1965.

[16] Whitfield, D. L. and High, H. D., "Velocity-Temperature Relations in Turbulent Boundary Layers with Nonunity Prandtl Numbers," *AIAA Journal*, Vol. 15, March 1977, pp. 431-434.

[17] Wu, J. M., Collins, F. G., and Bhat, M. K., "Final Report for NASA NSG 2379 Transonic Slotted Wind Tunnel Wall Boundary Layer Flow Study," NASA Ames Research Center, Moffett Field, Calif., Aug. 1982.

[18] Lighthill, M. J., "On Displacement Thickness," *Journal of Fluid Mechanics*, Vol. 4, Aug. 1958, p. 383.

[19] Perkins, H. H., "The Formation of Streamwise Vorticity in Turbulent Flow," *Journal of Fluid Mechanics*, Vol. 44, Dec. 1970, p. 721.